

## Spin Gap and Resonance at the Nesting Wave Vector in Superconducting FeSe<sub>0.4</sub>Te<sub>0.6</sub>

Yiming Qiu,<sup>1,2</sup> Wei Bao,<sup>3,\*</sup> Y. Zhao,<sup>4</sup> Collin Broholm,<sup>4,1</sup> V. Stanev,<sup>4</sup> Z. Tesanovic,<sup>4</sup> Y. C. Gasparovic,<sup>1,2</sup> S. Chang,<sup>1</sup> Jin Hu,<sup>5</sup> Bin Qian,<sup>5</sup> Minghu Fang,<sup>5,6</sup> and Zhiqiang Mao<sup>5</sup>

<sup>1</sup>*NIST Center for Neutron Research, National Institute of Standards and Technology, Gaithersburg, Maryland 20899, USA*

<sup>2</sup>*Department of Materials Science and Engineering, University of Maryland, College Park, Maryland 20742, USA*

<sup>3</sup>*Department of Physics, Renmin University of China, Beijing 100872, China*

<sup>4</sup>*Institute for Quantum Matter and Department of Physics and Astronomy, The Johns Hopkins University, Baltimore, Maryland 21218 USA*

<sup>5</sup>*Department of Physics, Tulane University, New Orleans, Louisiana 70118 USA*

<sup>6</sup>*Department of Physics, Zhejiang University, Hangzhou 310027, China*

(Received 12 May 2009; published 7 August 2009)

Neutron scattering is used to probe magnetic excitations in FeSe<sub>0.4</sub>Te<sub>0.6</sub> ( $T_c = 14$  K). Low energy spin fluctuations are found with a characteristic wave vector ( $\frac{1}{2}\frac{1}{2}L$ ) that corresponds to Fermi surface nesting and differs from  $\mathbf{Q}_m = (\delta 0\frac{1}{2})$  for magnetic ordering in Fe<sub>1+y</sub>Te. A spin resonance with  $\hbar\Omega_0 = 6.51(4)$  meV  $\approx 5.3k_B T_c$  and  $\hbar\Gamma = 1.25(5)$  meV develops in the superconducting state from a normal state continuum. We show that the resonance is consistent with a bound state associated with  $s_{\pm}$  superconductivity and imperfect quasi-2D Fermi surface nesting.

DOI: 10.1103/PhysRevLett.103.067008

PACS numbers: 74.70.-b, 74.20.Mn, 74.25.Ha, 78.70.Nx

The recent discovery of superconductivity in oxypnictides of the form  $R\text{FeAsO}$  (1111) [1] has triggered a burst of scientific activity. Subsequently reported superconductivity in suitably doped BaFe<sub>2</sub>As<sub>2</sub> (122) [2], LiFeAs [3], and FeSe (11) [4] indicates a crucial role for the shared FeAs or FeSe antiferromagnetic layer. The theoretical electronic structure is indeed dominated at the Fermi level by contributions from this layer [5] and density functional theory [6] successfully predicts, as a consequence of Fermi surface nesting, the observed antiferromagnetic order in the 1111 [7] and 122 type parent compounds [8,9]. In contrast, the magnetic parent compounds of 11-type superconductors order with a tunable antiferromagnetic vector  $\mathbf{Q}_m = (\delta 0\frac{1}{2})$  [10], with an in-plane component that is rotated by 45° with respect to the  $\mathbf{Q}_n = (\frac{1}{2}\frac{1}{2})$  nesting vector connecting the  $\Gamma$  and  $M$  points [see inset to Fig. 1(d)].

Recently, a spin resonance was discovered at the antiferromagnetic nesting vector in BaFe<sub>2</sub>As<sub>2</sub>-derived superconductors [11–13]. This raises several important questions: Does a spin resonance generally exist for the iron pnictide superconductor and for Fe(Se,Te) in particular, where in reciprocal space is it to be found? In this Letter we report that superconducting Fe(Se,Te) *does* exhibit a spin resonance though not at  $\mathbf{Q}_m$  but at the  $\Gamma - M$  Fermi surface nesting vector,  $\mathbf{Q}_n$ . This indicates a common form of superconductivity in the 122 and 11 families of iron based superconductors and brings into view a striking unifying feature of a wide range of unconventional superconductors proximate to magnetism: They exhibit a spin resonance at an energy  $\hbar\Omega_0$  that scales with  $k_B T_c$  [14] and a commensurate wave vector that reverses the sign of the superconducting order parameter.

Single crystals of FeSe<sub>0.4</sub>Te<sub>0.6</sub> were grown by a flux method. Growth methods and bulk properties are reported

elsewhere [15]. Bulk superconductivity in samples prepared as ours and labeled SC1 in Ref. [15] is indicated by sharp anomalies in resistivity, magnetic susceptibility and heat capacity with an onset at  $T_c \approx 14$  K. While the present experiment did not probe elastic magnetic scattering, there are no indications of a separate magnetic phase transition in bulk properties. The lattice parameters of the tetragonal  $P4/nmm$  unit cell are  $a = b = 3.802$  Å and

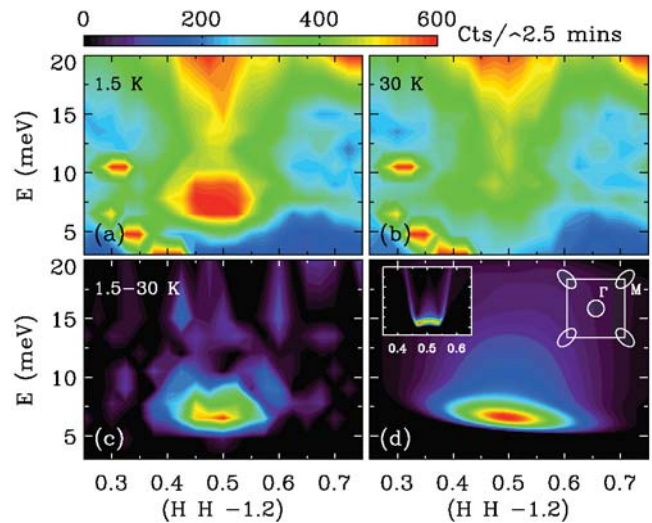


FIG. 1 (color). Spin excitation spectrum as a function of  $\mathbf{Q} = (H, H, -1.2)$  and energy at (a) 1.5 K and (b) 30 K. (c) The difference between the 1.5 K and 30 K spectra. The intensity in (c) is multiplied by a factor of 2 so that the same intensity scale at the top is used for (a)–(c). (d) Resolution convolved theoretical intensity difference from a simplified two-band model extracted from ARPES measurements [25]. The insets show the resolution free theoretical intensity difference (left) and the normal state Fermi surface employed (right).

$c = 6.061 \text{ \AA}$  at room temperature. Five crystals, weighing  $\sim 2 \text{ g}$  each, were mutually aligned to increase the count rate. The mosaic full width at half maximum (FWHM) of the individual samples and the coaligned assembly are 2.8 degrees and 4.8 degrees, respectively. Magnetic neutron scattering measurements were performed using thermal (BT7) and cold (SPINS) neutron triple-axis spectrometers at NIST. The sample temperature was controlled by a pumped  $^4\text{He}$  cryostat. As opposed to experiments on samples containing 8% excess Fe [10], no low energy magnetic signals were detected at the antiferromagnetic wave vector  $\mathbf{Q}_m = (\delta 0 \frac{1}{2})$  in  $\text{FeSe}_{0.4}\text{Te}_{0.6}$ . Therefore, we will concentrate on results from scans in the (*HHL*) reciprocal plane from BT7, using the fixed  $E_f = 14.7 \text{ meV}$  configuration. Measurements with better resolution and in a 7 T cryomagnet were conducted at SPINS using  $E_f = 4.2 \text{ meV}$ . Pyrolytic graphite (PG) and cooled Be were used to reject order contamination on BT7 and SPINS, respectively, and both instruments employ PG to monochromate the incident beam and analyze the scattered beam.

Figures 1(a) and 1(b) show the spin excitation spectrum of  $\text{FeSe}_{0.4}\text{Te}_{0.6}$ , combining 10 different constant energy scans near the in-plane nesting vector  $(\frac{1}{2} \frac{1}{2})$ , at temperature  $T = 1.5 \text{ K}$  and  $30 \text{ K}$ , respectively. The temperature independent, sharp spurions in (a) and (b) cancel in the difference spectrum [Fig. 1(c)]. An intense “resonance” sharply defined both in energy and in-plane momentum appears below  $T_c$ , above the normal state ridgelike continuum at the nesting vector  $\mathbf{Q}_n$  rather than at the wave vector  $\mathbf{Q}_m$  of the antiferromagnetic parent compound. Correspondingly we note that while the “parent” nonsuperconducting heavy fermion compound  $\text{CeRhIn}_5$  orders in an incommensurate antiferromagnetic structure [16], the resonance in superconducting  $\text{CeCoIn}_5$  appears at the commensurate wave vector associated with  $d_{x^2-y^2}$  superconductivity [17].

Figure 2(a) shows constant- $\mathbf{Q}$  scans through the resonance above and below  $T_c$ , together with measured background. The spectrum appears to be gapless in the normal state as measured at  $30 \text{ K}$  with a weak “knee” at the resonance energy. The normal state data in Fig. 1(b) is similar to data from paramagnetic and metallic  $\text{V}_2\text{O}_3$  (see Fig. 2(b) of Ref. [18]) indicating spin fluctuations resulting from Fermi surface nesting. At  $1.5 \text{ K}$ , a full spin gap is opened at low energies as spectral weight concentrates in a resonance peak at  $\hbar\Omega_0 = 6.51(4) \text{ meV}$ . Higher resolution constant- $\mathbf{Q}$  scans measured using cold neutrons are shown in Fig. 2(b). Here the SPINS spectrometer was arranged so the line of intensity from  $\mathbf{Q} = (0.5, 0.5, -0.796)$  to  $(0.5, 0.5, -1.804)$  was collected by the focusing analyzer during the scan. The resonance peak is much wider than the FWHM instrumental resolution,  $0.48 \text{ meV}$ . The resolution-corrected half width  $\hbar\Gamma = 1.25(5) \text{ meV}$  may indicate a finite lifetime of the resonant spin fluctuations, imperfect nesting, or broadening due to disorder on the Se/Te site.

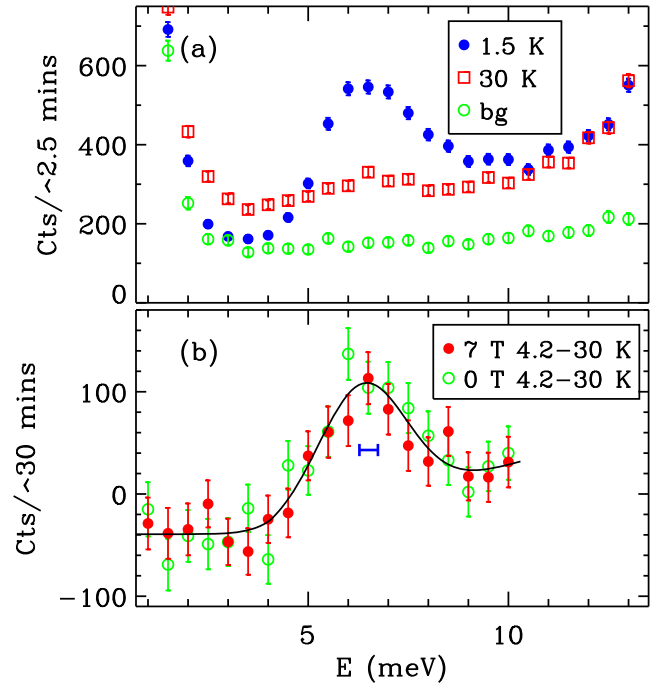


FIG. 2 (color online). (a) Constant  $\mathbf{Q} = (0.46, 0.46, 0.65)$  scan at  $1.5 \text{ K}$  and  $30 \text{ K}$ , measured at BT7. The sample-turned background measured at  $30 \text{ K}$  is shown by green open circles. (b) The difference intensity of the const- $\mathbf{Q} = (\frac{1}{2} \frac{1}{2} L)$  scans measured at  $4.2$  and  $30 \text{ K}$  using SPINS, with and without an applied  $7 \text{ T}$  magnetic field. The solid line is a guide to the eye. The blue bar indicates the FWHM instrumental energy resolution.

To determine the spatial correlations associated with the resonance, constant energy scans were performed in its vicinity. Figure 3(a) shows a basal plane scan at the resonance energy covering a full Brillouin zone. Weak intensity at  $\mathbf{Q} = (\frac{1}{2} \frac{1}{2} \frac{1}{2})$  and  $T = 30 \text{ K}$  is strongly enhanced in the superconducting state at  $T = 1.5 \text{ K}$ . The net enhancement is shown by the difference data in Fig. 3(c). Spurions exist at both temperatures but these cancel in the difference plot. The horizontal bar indicates the FWHM instrumental resolution. Based on the calculated resolution function, the deconvolved half width at half maximum is  $0.023(5) \times \sqrt{2} \times a^*$ , indicating a correlation length of  $19(4) \text{ \AA}$  or  $7(1)$  Fe-Fe lattice spacings. Figure 3(b) shows a scan in the interplane direction above and below  $T_c$ , with the difference in (d). As for quasi-two-dimensional  $\text{BaFe}_{1.84}\text{Co}_{0.16}\text{As}_2$  [12] but distinct from the more three-dimensional case of  $\text{BaFe}_{1.9}\text{Ni}_{0.1}\text{As}_2$  [13], the resonant spin correlations show no  $\mathbf{Q} \cdot \mathbf{c}$  dependence beyond that associated with the product of the Fe magnetic form factor squared and the varying projection of the instrumental resolution volume along  $\mathbf{c}$  (solid line).

Figure 4 shows the  $\hbar\omega - T$  dependence of magnetic scattering at the nesting vector. The spin resonance and the associated spin gap appear along with superconductivity for  $T < T_c = 14 \text{ K}$ . There is no detectable softening of

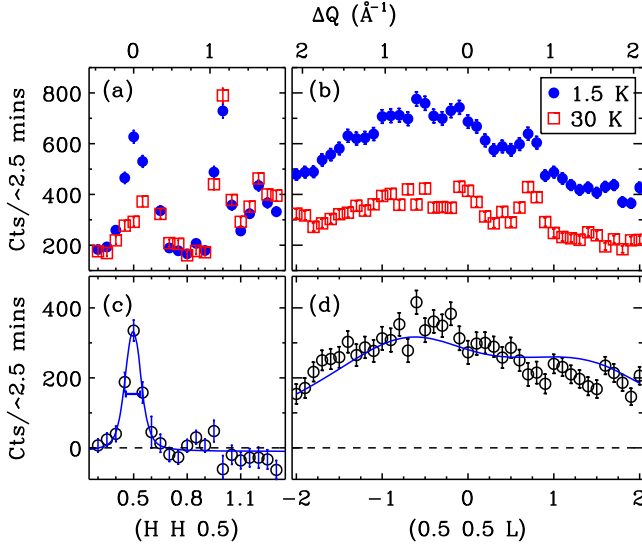


FIG. 3 (color online). Constant  $\hbar\omega = 6.5$  meV scans (a) along the  $(HH\frac{1}{2})$  direction, and (b) along the  $(\frac{1}{2}\frac{1}{2}L)$  direction, showing the quasi-two-dimensionality of the spin resonance. (c)–(d) The difference between the 1.5 K and 30 K scans. In (c) the solid line is a fit to a resolution convolved Lorentzian, and the horizontal bar represents the FWHM of the resolution. In (d) the line is the product of the Fe magnetic form factor squared and the projection of the instrumental resolution volume along  $c$ .

the resonance energy upon heating, indicating that it remains a characteristic energy scale in the normal state spectrum. In the inset, the temperature dependence of the integrated intensity of the resonance resembles an order parameter for the superconducting transition as in uncon-

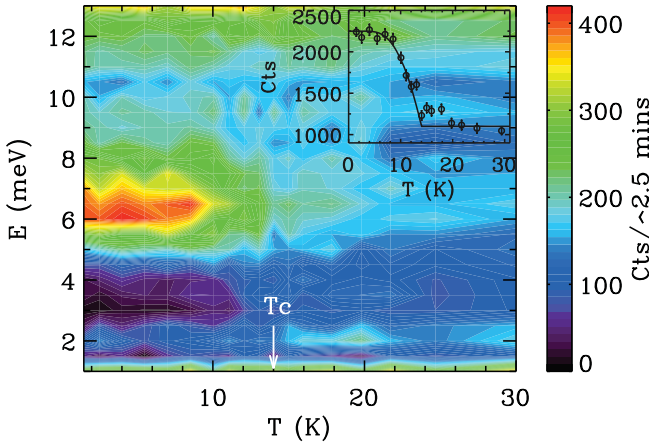


FIG. 4 (color). The energy scan at  $\mathbf{Q} = (0.46, 0.46, 0.66)$  as a function of temperature indicating association between the spin resonance and superconductivity in  $\text{FeSe}_{0.4}\text{Te}_{0.6}$ . The sample-turned background was subtracted from the data. The inset shows the integrated intensity of the resonance between 5 meV and 8 meV as a function of temperature, and the line is a fit to mean field theory with  $T_c = 14$  K.

ventional cuprate [19] and heavy fermion [17,20] superconductors. The ratio between the resonance energy and the superconducting transition temperature  $\hbar\Omega_0/k_B T_c = 5.3$  for our  $\text{FeSe}_{0.4}\text{Te}_{0.6}$  sample is larger than 2–4 reported for heavy fermion superconductors [17,20], 4.3 for  $\text{Ba}_{0.6}\text{K}_{0.4}\text{Fe}_2\text{As}_2$  [11] and 4.5 for  $\text{BaFe}_{1.84}\text{Co}_{0.16}\text{As}_2$  [12], but comparable to the canonical value of 5 for cuprate superconductors [21]. It also follows a general trend for a wide range of quantum condensation phenomena [14].

Turning now to the theoretical interpretation of the data, we note that the  $\mathbf{Q}$  and  $E$  dependent  $\chi''(\mathbf{Q}, E)$  measured through magnetic neutron scattering in the superconducting state reflects the symmetry of the superconducting gap function [22]. Because of the emblematic  $s_{\pm}$  coherence factors for the interband processes,  $1 + \frac{\Delta^2}{E_q^2}$ , the creation of a pair of Bogoliubov–de Gennes (BdG) quasiparticles is *enhanced*, in contrast to being suppressed as in a conventional  $s$ -wave state, where the corresponding coherence factor is  $1 - \frac{\Delta^2}{E_q^2}$  [23]. This leads to a divergence in the imaginary part of  $\chi_0(\mathbf{Q}_n, E \rightarrow 2\Delta)$  [24]. In addition, interactions pull the resonant peak below  $2\Delta$ , creating a “bound state” of two BdG quasiparticles within the superconducting gap.

We now demonstrate that this rather simple theoretical picture is consistent with the present data. The explicit calculation employs an RPA-type scheme and uses a two-band model, with one hole and one electron parabolic 2D bands [inset to Fig. 1(d)]. The band parameters are from ARPES measurements [25]. The position of the resonance is mainly controlled by the strength of the interaction while the eccentricity determines its width in  $\mathbf{Q}$ —extracting those parameters from the fits is a well-defined procedure. Here we use  $2\Delta_0 = 7.5$  meV ( $2\Delta_0/k_B T_c \approx 6.1$ ), higher than the BCS value but within the range measured in pnictides [26]. The eccentricity of the electron band is around 0.83, the interaction strength is set to 0.3 in units of inverse density of states (DOS), and areas of the hole and the electron pockets are roughly similar. More generally, reasonable fits are obtained for eccentricity and interaction in the ranges 0.83–0.90 and 0.26–0.34, respectively. Following the standard procedure, a small fixed imaginary part ( $\approx 0.1\Delta_0$ ) was added to  $\omega$  to smooth out the numerics. For comparison to Fig. 1(c) we subtracted the theoretical 30 K normal state intensity and convolved with the instrumental resolution. The result captures the essential physics of the resonance, as shown in Fig. 1(d).

The main insight gained by this calculation is that the good fit to the observed shape and position of the resonance necessarily calls for significant deviations from perfect nesting. In agreement with the ARPES data, we find best fits for a circular hole band and an elliptical electron band. This explains the absence of an antiferromagnetic spin-density-wave (SDW) ordering along the “nesting” vector in the normal state [10]—the peak in the spin susceptibility is highly sensitive to deviations from perfect nesting [27]

and the combination of a depressed peak and better-screened interactions can readily destabilize the SDW state. Overall, the above calculation supports the  $s_{\pm}$  superconducting state and the notion that superconductivity sets in after the itinerant SDW order has been suppressed by deviations from perfect nesting.

Since the discovery of the spin resonance in cuprate superconductors [19], there has been much debate on whether it is associated with an intrinsic influence of superconductivity on spin correlations, or with a pre-existing collective mode of a nearby magnetic order enhanced by the loss of electron-hole pair damping in the superconducting state [21]. According to the former scenario and the theory described above, the resonance should be a triplet—splitting linearly in an applied field. To determine the spin space multiplicity of the resonance, we carried out a constant- $\hbar\omega$  scan in a field of 7 Tesla. No splitting is directly visible in the data shown in Fig. 2(b). Fitting these data to a triplet (doublet) places an upper limit of 1.3 meV (1.2 meV) on the overall level spacing. For comparison, Zeeman splitting of a spin multiplet with  $g = 2$  would amount to  $g\mu_B H = 0.81$  meV. Higher fields may help to overcome the zero field broadening and determine the multiplicity of the resonance.

In summary, we observe a strong quasi-two-dimensional spin resonance at the energy  $\hbar\Omega_0 = 6.5$  meV and the wave vector  $\mathbf{Q}_n = (\frac{1}{2}, \frac{1}{2}, L)$  in superconducting  $\text{FeSe}_{0.4}\text{Te}_{0.6}$ . The peak has finite half widths in momentum and energy of  $0.06(1) \text{ \AA}^{-1}$  and  $\hbar\Gamma = 1.25(5)$  meV, respectively. These experimental results are consistent with theoretical predictions for a  $s_{\pm}$  superconducting pairing function [23,24,27]. Despite a different critical wave vector  $\mathbf{Q}_m$  in the antiferromagnet parent compound  $\text{Fe}_{1+y}\text{Te}$ , imperfect nesting of hole and electron Fermi surfaces separated by  $\mathbf{Q}_n$  appears to lie behind  $s_{\pm}$  superconductivity in  $\text{FeSe}_{0.4}\text{Te}_{0.6}$  as in the other Fe-based superconductors.

Work at Tulane was supported by the NSF under Grant No. DMR-0645305 for materials, the DOE under DE-FG02-07ER46358 for graduate students, and by the Research Corporation. Work at JHU was supported by the DOE under DE-FG02-08ER46544. Work at ZU was supported by the NBRP of China (No. 2006CB01003, 2009CB929104) and the PCSIRT of the MOE of China (IRT0754). SPINS is in part supported by NSF under agreement DMR-0454672.

*Note added.*—After completing our experiments at BT7 and SPINS on March 9, 2009, a related preprint describing neutron scattering experiments on a mixture of  $\text{FeSe}_{0.45}\text{Te}_{0.55}$  and  $\text{FeSe}_{0.65}\text{Te}_{0.35}$  came to our attention [28].

---

\*wbao@ruc.edu.cn

- [1] Y. Kamihara *et al.*, J. Am. Chem. Soc. **130**, 3296 (2008); X.H. Chen *et al.*, Nature (London) **453**, 761 (2008); G.F. Chen *et al.*, Phys. Rev. Lett. **100**, 247002 (2008); Z. A. Ren *et al.*, Chin. Phys. Lett. **25**, 2215 (2008); H.H. Wen *et al.*, Europhys. Lett. **82** 17009 (2008); C. Wang *et al.*, *ibid.* **83**, 67006 (2008).
- [2] M. Rotter *et al.*, Phys. Rev. Lett. **101**, 107006 (2008); G.F. Chen *et al.*, Chin. Phys. Lett. **25**, 3403 (2008); K. Sasmal *et al.*, Phys. Rev. Lett. **101**, 107007 (2008); M. S. Torikachvili *et al.*, *ibid.* **101**, 057006 (2008); G. Wu *et al.* Europhys. Lett. **84**, 27010 (2008).
- [3] X. Wang *et al.*, Solid State Commun. **148**, 538 (2008); J.H. Tapp *et al.*, Phys. Rev. B **78**, 060505(R) (2008); M.J. Pitcher *et al.*, Chem. Commun. (Cambridge) 45 (2008) 5918.
- [4] F.-C. Hsu *et al.*, Proc. Natl. Acad. Sci. U.S.A. **105**, 14262 (2008); M.H. Fang *et al.*, Phys. Rev. B **78**, 224503 (2008).
- [5] D.J. Singh, Physica (Amsterdam) **469C**, 418 (2009).
- [6] F. Ma and Z. Y. Lu, Phys. Rev. B **78**, 033111 (2008); J. Dong *et al.*, Europhys. Lett. **83**, 27006 (2008).
- [7] C. de la Cruz *et al.*, Nature (London) **453**, 899 (2008); M. A. McGuire *et al.*, Phys. Rev. B **78**, 094517 (2008)
- [8] Q. Huang *et al.*, Phys. Rev. Lett. **101**, 257003 (2008).
- [9] A. Goldman *et al.*, Phys. Rev. B **78**, 100506(R) (2008).
- [10] W. Bao *et al.*, Phys. Rev. Lett. **102**, 247001 (2009).
- [11] A. D. Christianson *et al.*, Nature (London) **456**, 930 (2008).
- [12] M. D. Lumsden *et al.*, Phys. Rev. Lett. **102**, 107005 (2009).
- [13] S. Chi *et al.*, Phys. Rev. Lett. **102**, 107006 (2009); S. Li *et al.*, Phys. Rev. B **79**, 174527 (2009).
- [14] Y. J. Uemura, Nature Mater. **8**, 253 (2009).
- [15] T. Liu *et al.*, arXiv:0904.0824.
- [16] W. Bao *et al.*, Phys. Rev. B **62**, R14621 (2000); **67**, 099903 (E) (2003).
- [17] C. Stock *et al.*, Phys. Rev. Lett. **100**, 087001 (2008).
- [18] W. Bao *et al.*, Phys. Rev. Lett. **78**, 507 (1997).
- [19] J. Rossat-Mignod *et al.*, Physica (Amsterdam) **185–189C**, 86 (1991); H. A. Mook *et al.*, Phys. Rev. Lett. **70**, 3490 (1993); H. F. Fong *et al.*, Nature (London) **398**, 588 (1999); H. F. He *et al.*, Science **295**, 1045 (2002).
- [20] N. Metoki *et al.*, Phys. Rev. Lett. **80**, 5417 (1998); O. Stockert *et al.*, Physica (Amsterdam) **403B**, 973 (2008).
- [21] P. Bourges *et al.*, Physica (Amsterdam) **424C**, 45 (2005).
- [22] R. Joynt and T. M. Rice, Phys. Rev. B **38**, 2345 (1988).
- [23] I. I. Mazin and J. Schmalian, Physica (Amsterdam) **469C**, 614 (2009).
- [24] M. M. Korshunov and I. Eremin, Phys. Rev. B **78**, 140509 (R) (2008); T. Maier and D. Scalapino, *ibid.* **78**, 020514 (R) (2008).
- [25] Y. Xia *et al.*, Phys. Rev. Lett. **103**, 037002 (2009).
- [26] L. Zhao *et al.*, Chin. Phys. Lett. **25**, 4402 (2008); H. Ding *et al.*, Europhys. Lett. **83**, 47001 (2008).
- [27] V. Cvetkovic and Z. Tesanovic, Europhys. Lett. **85**, 37002 (2009).
- [28] H. A. Mook *et al.*, arXiv:0904.2178.